

## ORIGINAL ARTICLE

# Contribution of ammonia oxidation to chemoautotrophy in Antarctic coastal waters

Bradley B Tolar<sup>1,2,5</sup>, Meredith J Ross<sup>1</sup>, Natalie J Wallsgrove<sup>3</sup>, Qian Liu<sup>1</sup>, Lihini I Aluwihare<sup>4</sup>, Brian N Popp<sup>3</sup> and James T Hollibaugh<sup>1</sup><sup>1</sup>Department of Marine Sciences, University of Georgia, Athens, GA, USA; <sup>2</sup>Department of Microbiology, University of Georgia, Athens, GA, USA; <sup>3</sup>Department of Geology and Geophysics, University of Hawai'i, Honolulu, HI, USA and <sup>4</sup>Scripps Institution of Oceanography, UC San Diego, La Jolla, CA, USA

There are few measurements of nitrification in polar regions, yet geochemical evidence suggests that it is significant, and chemoautotrophy supported by nitrification has been suggested as an important contribution to prokaryotic production during the polar winter. This study reports seasonal ammonia oxidation (AO) rates, gene and transcript abundance in continental shelf waters west of the Antarctic Peninsula, where Thaumarchaeota strongly dominate populations of ammonia-oxidizing organisms. Higher AO rates were observed in the late winter surface mixed layer compared with the same water mass sampled during summer (mean  $\pm$  s.e.:  $62 \pm 16$  versus  $13 \pm 2.8$  nM per day, *t*-test  $P < 0.0005$ ). AO rates in the circumpolar deep water did not differ between seasons ( $21 \pm 5.7$  versus  $24 \pm 6.6$  nM per day;  $P = 0.83$ ), despite 5- to 20-fold greater Thaumarchaeota abundance during summer. AO rates correlated with concentrations of Archaea ammonia monooxygenase (*amoA*) genes during summer, but not with concentrations of Archaea *amoA* transcripts, or with ratios of Archaea *amoA* transcripts per gene, or with concentrations of Betaproteobacterial *amoA* genes or transcripts. The AO rates we report ( $< 0.1$ – $220$  nM per day) are  $\sim 10$ -fold greater than reported previously for Antarctic waters and suggest that inclusion of Antarctic coastal waters in global estimates of oceanic nitrification could increase global rate estimates by  $\sim 9\%$ . Chemoautotrophic carbon fixation supported by AO was 3–6% of annualized phytoplankton primary production and production of Thaumarchaeota biomass supported by AO could account for  $\sim 9\%$  of the bacterioplankton production measured in winter. Growth rates of thaumarchaeote populations inferred from AO rates averaged 0.3 per day and ranged from 0.01 to 2.1 per day.

The ISME Journal (2016) 10, 2605–2619; doi:10.1038/ismej.2016.61; published online 17 May 2016

## Introduction

Polar oceans are subject to strong seasonal variation in primary production, driven by the seasonal cycle of irradiance, vertical mixing and ice cover. The near absence of photoautotrophic production at high latitudes during winter raises the question of how the marine food web, and especially the marine microbial food web, functions during this period of greatly reduced supply of phytoplankton-derived, labile organic carbon. Heterotrophy based on the consumption of moderately recalcitrant dissolved organic carbon stocks built up during the highly productive summer season has been considered as one possibility for supporting the Antarctic winter food web (Azam *et al.*, 1991). Chemoautotrophic production has also

been suggested to account for prokaryotic production in Antarctic waters during winter (Manganelli *et al.*, 2009), with nitrification as a likely metabolism (Grzymski *et al.*, 2012; Williams *et al.*, 2012).

Ammonia oxidation (AO) rates have been measured in most oceans and range from 0 to 100 nM per day (reviewed in Yool *et al.*, 2007; Ward, 2008, 2011); however, there are few measurements of AO rates from polar regions. Arctic data are limited to a small number of potential rate measurements (addition of  $1 \mu\text{M}$   $^{15}\text{NH}_4\text{Cl}$  tracer) made on samples collected off Barrow, AK (Christman *et al.*, 2011). Southern Ocean data are limited to a handful of sites (Olson 1981a, b; Bianchi *et al.*, 1997) and to depths  $\leq 100$  m, although thaumarchaeotes are abundant in both Arctic (Kalanetra *et al.*, 2009, Christman *et al.*, 2011) and Antarctic (DeLong *et al.*, 1994; Massana *et al.*, 1998; Murray *et al.*, 1998, 1999; Church *et al.*, 2003; Kalanetra *et al.*, 2009; Alonso-Sáez *et al.*, 2011) waters and geochemical evidence suggests significant nitrification in the Antarctic winter mixed layer (Smart *et al.*, 2015).

The waters of the Antarctic continental shelf West of the Antarctic Peninsula (WAP hereinafter; Supplementary Figure 1a) are characterized by the

Correspondence: JT Hollibaugh, Department of Marine Sciences, University of Georgia, 248 Marine Sciences Building, Athens, GA 30602, USA.

E-mail: aquadoc@uga.edu

<sup>5</sup>Current address: Department of Earth System Science, Stanford University, Stanford, CA, USA.

Received 25 August 2015; revised 4 February 2016; accepted 22 March 2016; published online 17 May 2016

strong seasonal and interannual variation in irradiance, sea ice cover and phytoplankton biomass and production (Ducklow *et al.*, 2007, 2012) that are typical of polar regions. The region has been studied intensively by the Palmer LTER (PAL-LTER; <http://pal.lternet.edu/>) since 1990. Water column stratification varies strongly by season (Hofmann and Klinck, 1998; Ducklow *et al.*, 2007; Martinson *et al.*, 2008). Using terminology from Church *et al.* (2003), the winter water column is stratified into two distinct water masses: (1) Antarctic surface water (AASW); and (2) circumpolar deep water (CDW). The surface mixed layer (AASW) extends from the surface to depths of 100–150 m, is colder ( $-1.8$  °C to  $-0.3$  °C) and less saline (salinity 33.3 to 34.3) than the CDW below it (Supplementary Figure 1b). The CDW is found at depths  $>150$  m year-round, and has temperatures ranging between  $0.2$  °C to  $2$  °C and salinities ranging from 34.4 to 34.7 (Supplementary Figure 1b). The AASW stratifies into two layers during summer as a result of warming and meltwater input, resulting in three water masses in the summer, coastal water column: (1) summer surface water (SSW, temperature  $0.5$  °C to  $1.5$  °C, salinity  $<33.8$ , depth 0–50 m); (2) WW (the remainder of the winter mixed layer at depths of 50–150 m); and (3) CDW (Supplementary Figures 1b and c).

Planktonic Archaea are most abundant in the upper water column of this region (AASW) during winter (May–November) and their population is dominated by Thaumarchaeota (Murray *et al.*, 1998; Church *et al.*, 2003; Grzymalski *et al.*, 2012). Archaeal abundance decreases during the transition from winter to summer. These reductions are most significant at the surface, with very few Archaea (1–2% of the population of prokaryotes) remaining in the SSW, as compared with higher abundances in the WW (5–10%) and CDW (13–17%) (Murray *et al.*, 1998; Church *et al.*, 2003).

Different microbial communities inhabit the three summer water masses (Massana *et al.*, 1998; Murray *et al.*, 1998; Church *et al.*, 2003) and a survey of summer populations of Thaumarchaeota reported lower abundances of Archaea *amoA* and lower ratios of Archaea *amoA* to Archaea 16S rRNA genes (*rrs*) in WW than in CDW samples (Kalanetra *et al.*, 2009). This suggested functional differentiation of Thaumarchaeota populations in these two water masses, accompanying (or possibly driving) phylogenetic differentiation of the populations, which is also observed (Kalanetra *et al.*, 2009; Alonso-Sáez *et al.*, 2011). We hypothesized that AO rate might be affected by community composition at the level of Thaumarchaeota ecotypes, as well as by their abundance. Thaumarchaeota diversity was characterized using high-throughput sequencing of *rrs* and *amoA* genes, which allowed robust comparisons of assemblage composition by season, as well as by location and depth, across nearly the entire WAP region. We sampled during late winter and the following summer to determine if the composition

of Thaumarchaeota populations changed during the evolution of ASW into summer surface water and WW.

We measured AO rates at multiple depths in continental shelf and slope waters west of the Antarctic Peninsula. We used the measured rates to estimate chemoautotrophic carbon fixation and the potential contribution of AO to bacterioplankton production during winter, as well as the growth rates of thaumarchaeote populations. We compared the AO rates to measurements of gene and transcript abundance with the aim of determining whether rates could be predicted from molecular data. We measured biogenic silica concentrations and diatom 18S rRNA gene abundance to test a hypothesis that Thaumarchaeota distributions in the WAP are coupled to ammonia regeneration from sinking diatom blooms. We also measured the abundance of *Nitrospina*—a prominent group of nitrite-oxidizing Bacteria—to investigate coupling between these two guilds of nitrifying microorganisms. We quantified Thaumarchaeota urease (*ureC*) genes in our samples, as their presence has been proposed (Yakimov *et al.*, 2011; Alonso-Sáez *et al.*, 2012; Connelly *et al.*, 2014; Pedneault *et al.*, 2014) to indicate a role for urea in nitrification and urea use might be tied to the vertical differentiation of Thaumarchaeota populations reported previously (Kalanetra *et al.*, 2009; Alonso-Sáez *et al.*, 2011).

## Materials and methods

### Sample collection

Samples were collected from the ARSV *Laurence M Gould* during late winter (17–24 September 2010; LMG 10-06; LTER 600 line only) and summer (7–30 January 2011; LMG 11-01, entire WAP region). Stations were located on the Antarctic continental shelf and slope west of the Antarctic Peninsula (Supplementary Figure 1a and Supplementary Table 1) within the PAL-LTER sampling domain (<http://pal.lternet.edu/>). Sampling focused on the AASW and CDW in late winter and WW and CDW in summer (depths sampled were  $<500$  m; Supplementary Table 1). We did not sample summer surface water as previous work (Church *et al.*, 2003; Kalanetra *et al.*, 2009) revealed very low Thaumarchaeota populations in this water mass. Water samples were collected from Go-Flo bottles (General Oceanics Inc., Miami, FL, USA) into opaque HDPE plastic bottles as soon as the rosette was secured on deck. Subsequent processing took place in an adjacent darkened laboratory. RNA samples were filtered immediately, placed in Whirl-pak bags (Nasco, Fort Atkinson, WI, USA), RNAlater (Ambion, Austin, TX, USA) was added, and then they were immediately frozen at  $-80$  °C ( $<15$  min after sample collection). DNA samples were filtered through  $0.22$   $\mu$ m pore size Sterivex GVWP filters (EMD Millipore, Billerica, MA, USA), 1.8 ml of lysis buffer (0.75 M sucrose, 40 mM EDTA, 50 mM Tris, pH 8.3) was added, and then the

samples were frozen at  $-80^{\circ}\text{C}$  within 30 min of sample collection. Nutrient samples were collected from the Sterivex filtrate, frozen at  $-20^{\circ}\text{C}$  and subsequently analyzed using standard methods:  $\text{NH}_4^+$  (Solórzano, 1969);  $\text{NO}_2^-$  and  $\text{NO}_3^-$  (Strickland and Parsons, 1972; Jones, 1984). Biogenic silica samples were collected on  $0.6\ \mu\text{m}$  pore size, 47 mm diameter, polycarbonate filters using a polycarbonate filter holder, placed in Whirl-pak bags that were frozen at  $-20^{\circ}\text{C}$  and subsequently analyzed as described in Brzezinski *et al.* (1997).

#### DNA and RNA analyses

DNA was recovered from frozen filters using a lysozyme and proteinase K digestion, followed by purification using a phenol–chloroform extraction following Bano and Hollibaugh (2000). Relative abundances of Archaea, Bacteria and diatom genes were determined using either SYBR Green I dye (BioRad, Hercules, CA, USA) or TaqMan (Applied Biosystems, Carlsbad, CA, USA) chemistries following published protocols (Kalanetra *et al.*, 2009; Tolar *et al.*, 2013) and the primers and probes listed in Supplementary Table 2. Quantitative PCR (qPCR) used an iCycler iQTM Real-Time qPCR detection system (BioRad). Reactions were set up in triplicate and analyzed against a range of standards ( $10^1$ – $10^7$  copies per  $\mu\text{l}$ ) as described in Tolar *et al.* (2013). qPCR conditions for Archaea *amoA*, ammonia-oxidizing Betaproteobacteria *amoA* and Bacteria *rrs* genes have been described previously (Kalanetra *et al.*, 2009; Tolar *et al.*, 2013). Thaumarchaeota *ureC* genes were quantified under the same conditions as *amoA*, with an annealing temperature of  $53^{\circ}\text{C}$  (from Alonso-Sáez *et al.*, 2012). *Nitrospina rrs* genes were quantified as in Mincer *et al.* (2007) and diatom 18S rRNA genes were quantified as described in Nguyen *et al.* (2011) and Baldi *et al.* (2011).

RNA was extracted from filters as described in Poretsky *et al.* (2005) and Gifford *et al.* (2011) with the substitution of 200- $\mu\text{m}$ -diameter zirconium beads (OPS Diagnostics, Lebanon, NJ, USA) in the initial bead-beating step and a final extract volume of 100  $\mu\text{l}$ . DNA was removed from 30  $\mu\text{l}$  of the RNA extract using the TURBO DNase-Free Kit (Ambion) following the manufacturer's instructions with a second enzyme treatment at  $2\times$  concentration. *amoA* transcripts from Archaea and Bacteria were quantified as above using the iScript One-Step RT-qPCR Kit with SYBR Green (BioRad) and an additional 10 min reverse transcription step at  $50^{\circ}\text{C}$  at the beginning of each run.

Raw abundance data (copies per  $\mu\text{l}$  of DNA or RNA extract) were converted to concentrations (copies per liter) of genes or transcripts using the volume filtered and the extract volume and assuming 100% extraction efficiency as in Tolar *et al.* (2013). The percent of total prokaryotes represented by Thaumarchaeota was calculated using *rrs* gene abundance (Bacteria plus Thaumarchaeota) determined by qPCR and corrected using an average of 1.8 Bacteria *rrs* genes per genome

(Biers *et al.*, 2009) and 1.0 Thaumarchaeota *rrs* gene per genome, as described previously (Kalanetra *et al.*, 2009). Prokaryote abundance determined by qPCR correlated well with total prokaryote counts made with a flow cytometer by Palmer LTER personnel during LMG 11-01 (slope = 0.87; 95% confidence interval = 0.52–1.22; Supplementary Figure 2).

#### Archaeal diversity

Samples for high-throughput sequencing were amplified in triplicate using primers 517Fa and 1058R (Archaea *rrs*; VAMPS project—<http://vamps.mbl.edu/resources/primers.php>) or CamoA-19f and CamoA-616r (Archaea *amoA*; Pester *et al.*, 2012). The first of the five 517F primers used by the VAMPS project to sequence the Archaea v6-v4 region was found to amplify 93.3% of Marine Group I Archaea and only 11% of Euryarchaeota (with no mismatches allowed), and so was selected for use (Supplementary Table 2). PCR reactions were pooled, purified and quantified, and then modified with Titanium (Lib-L) adaptors and sample-specific barcodes. Tagged amplicons were pooled in equimolar concentrations and submitted for sequencing on a Roche 454 GS-FLX instrument (454 Life Sciences, Branford, CT, USA) with Titanium chemistry maintained by the Georgia Genomics Facility (University of Georgia, Athens, GA, USA). Postsequencing processing of reads followed the Schloss laboratory 454 SOP ([http://www.mothur.org/wiki/454\\_SOP](http://www.mothur.org/wiki/454_SOP); Schloss *et al.*, 2011, last accessed January 2014).

#### AO rates

AO rates were measured in 96 h incubations at  $0^{\circ}\text{C}$  in the dark using  $^{15}\text{N}$ -labeled ammonium ( $>99\%$   $^{15}\text{NH}_4\text{Cl}$ ; Cambridge Isotope Laboratories, Tewksbury, MA, USA) added at 50 nM (Santoro *et al.*, 2010; Beman *et al.*, 2012) to 200 ml samples contained in acid-washed, sample-rinsed, polycarbonate bottles that were wrapped in aluminum foil, enclosed in cardboard boxes and placed in a dark Percival incubator (Perry, IA, USA). The 50 nM additions were 0.9–93% (median 4.5%) of *in situ* ammonium concentrations, with only 9 of 66 samples receiving  $>10\%$  enrichment and only 2 samples receiving  $>50\%$  enrichments (Supplementary Table 1). There was no statistically significant correlation between AO rate and ammonium enrichment factor for the complete data set. Nine of the 10 samples where enrichments were  $>10\%$  were from summer CDW samples. The mean  $\pm$  s.e. of AO rates for these samples was  $16.6 \pm 3.8$  versus  $17.6 \pm 3.3$  nM per day for the rest of the summer CDW samples; however, the difference between these subsets was not statistically significant (two-tailed *t*-test,  $P=0.84$ ). Treatments were run in duplicate for each sample with a single blank consisting of either filtered sample seawater (Sterivex filtrate) or a subsample frozen at  $-80^{\circ}\text{C}$  immediately after tracer addition. Incubations were terminated by removing 50 ml

subsamples from each bottle that were immediately frozen at  $-80^{\circ}\text{C}$ .

The  $^{15}\text{NO}_x$  produced in the incubations was measured using the 'denitrifier method' (Sigman *et al.*, 2001) as described in Popp *et al.* (1995), Dore *et al.* (1998) and Beman *et al.* (2011). We calculated AO rates from  $\delta^{15}\text{N}$  values of the  $\text{NO}_x$  pool as described previously (Beman *et al.*, 2008; Christman *et al.*, 2011). Means of the duplicates are reported in Supplementary Table 1. Rates calculated for each replicate assay from a sample differed by  $>50\%$  of the mean in 16 of 66 samples. These are flagged in Supplementary Table 1, but were retained in the analyses presented below.

We ran time-course incubations with samples taken from two depths (WW and CDW) at two stations to verify that oxidation rates did not change significantly, for example, due to substrate depletion or growth of ammonia oxidizers, during the 96 h incubations. These experiments were set up in 250 ml bottles as above, with six sets of two treatments plus one filtered seawater blank (18 bottles) per sample. Two treatment bottles and one blank were sacrificed at each of six time points taken over time courses of 139 and 181 h. These data are presented in Supplementary Table 3. AO rates were determined from the slope of linear regressions of the data from a given sample. Although the difference between replicates was  $>50\%$  for some pairs of replicates, which were discarded for the calculation of AO rates from these time courses, there was no indication that rates changed during the course of these prolonged incubations.

#### Statistical analysis

Principal components analysis (PCA) and non-metric multidimensional scaling (NMDS) were performed in R (<http://www.r-project.org/>) using the *prcomp* (stats package; PCA), *metaMDS* (vegan package; NMDS) and *lm* (stats package; pairwise linear regression) commands as in Hollibaugh *et al.* (2014). PCA analysis was run separately on LMG 11-01 and LMG 10-06 data sets to include variables not collected during LMG 10-06 (turbidity, dissolved oxygen, biogenic silica) and to reduce bias from oversampling along the LTER 600 line. A correlation matrix was used for PCA as the variance for all environmental variables was set to 1 (using the option 'scale. = TRUE' in R). The *metaMDS* command in R runs a PCA after NMDS to rectify the axes such that the first axis explains the most variation, followed by the second axis, and so on. We compare each PCA axis to both rectified NMDS axes (thus to the entire NMDS data set), but only found significant relationships with NMDS axis 1. Temperature and salinity were used to calculate sigma-t to identify water masses, and  $\text{NO}_2^-$  and  $\text{NO}_3^-$  were summed as  $\text{NO}_x$  for LMG 11-01. Both qPCR-estimated gene abundances and the distribution of *rrs* and *amoA* sequences among 454-generated operational taxonomic units (OTUs) were used in NMDS analysis (separately). An analysis of molecular variance (Excoffier *et al.*, 1992), run in R,

was used to test the significance of differences in community composition between samples. Student's *t*-tests and Pearson's product-moment correlations were also performed in R using the *t.test* and *cor.test* commands (stats package), respectively. Model II regressions were calculated using the *lmodel2* package (Legendre and Legendre, 1998) in R with major axis regressions.

#### Data sets

DNA sequences obtained by high-throughput sequencing have been deposited with Genbank in the SRA archive under study PRJNA268106, accession number SRP050086. Nutrient, qPCR and AO rate data have been deposited with the Antarctic Master Directory at <http://gcmd.nasa.gov/getdif.htm?NSF-ANT08-38996> and a summary is presented in Supplementary Table 1.

## Results

#### Environmental characteristics

Environmental data are summarized in Table 1 (all data are presented in Supplementary Table 1). PCA of the characteristics of samples taken during summer explained 52.3% (axes PC1 plus PC2) of the total variation in the data set and supported division of samples into WW and CDW water masses (Supplementary Figure 3a), consistent with their characterization based solely on temperature and salinity (Supplementary Figure 1b). The samples did not segregate by sampling location (onshore versus offshore, north versus south). A PCA run on the subset of samples used for high-throughput sequencing demonstrated the same separation of WW and CDW samples as that run for all summer samples (data not shown).

#### AO rates

AO rates ranged from  $<0.1$  (limit of detection) to 220 nM per day. Late winter AO rates in AASW were not significantly different from rates in late winter CDW samples (Table 2, means  $\pm$  s.e.:  $62 \pm 16$  versus  $21 \pm 5.7$  nM per day, respectively; Student's *t*-test  $P=0.11$ ). AO rates in the LAASW (the precursor to WW) were significantly higher compared with that in the WW ( $79 \pm 30$  and  $13 \pm 2.8$  for LAASW versus WW,  $P=0.0003$ ). However, rates in WW samples were not significantly different from rates in summer CDW samples (Table 2;  $13 \pm 2.8$  versus  $24 \pm 6.6$  nM per day;  $P=0.14$ ).

#### Thaumarchaeota gene and transcript abundance

Thaumarchaeota were detected at all stations and depths sampled on both cruises (Supplementary Table 1), with abundance ranging from  $1.3 \times 10^4$  to  $6.5 \times 10^7$  cells per liter (estimated from *amoA*) and  $3.6 \times 10^2$  to  $3.0 \times 10^7$  cells per liter (from *rrs*).

**Table 1** Summary of environmental variables measured in the water masses sampled for this study

Water mass	Depth range (m)	Temp (°C)	Salinity (PSU)	Chl a (mg m <sup>-3</sup> )	Dissolved oxygen (mg l <sup>-1</sup> )	NO <sub>2</sub> <sup>-</sup> (µM)	NO <sub>3</sub> <sup>-</sup> (µM)	NH <sub>4</sub> <sup>+</sup> (µM)	Biogenic silicate (µM)	
UAASW (winter)	10	Max	-1.76	33.97	0.1	ND	0.2	36.9	1.0	ND
		Min	-1.84	33.90	0.1	ND	0.1	25.7	0.4	ND
		Mean	-1.80	33.93	0.1	ND	0.2	31.2	0.7	ND
		s.e.	0.02	0.01	0.00	ND	0.02	1.6	0.10	ND
LAASW (winter)	55–75	Max	-0.82	34.13	0.1	ND	0.2	36.5	1.1	ND
		Min	-1.83	33.91	0.1	ND	0.1	30.1	0.6	ND
		Mean	-1.62	33.97	0.1	ND	0.2	32.4	0.7	ND
		s.e.	0.16	0.03	0.01	ND	0.01	0.9	0.08	ND
CDW (winter)	260–300	Max	2.09	34.68	0.1	ND	0.2	38.3	1.1	ND
		Min	1.32	34.61	0.1	ND	0.0	29.6	0.5	ND
		Mean	1.55	34.64	0.1	ND	0.1	34.8	0.9	ND
		s.e.	0.11	0.01	0.001	ND	0.02	1.2	0.09	ND
WW (summer)	70–125	Max	0.27	34.03	1.5	8.4	0.3	32.5	5.6	1.4
		Min	-1.77	33.83	0.0	6.5	0.1	13.8	0.6	0.0
		Mean	-1.05	33.94	0.5	7.6	0.2	27.1	2.1	0.2
		s.e.	0.10	0.01	0.09	0.07	0.01	0.9	0.26	0.09
CDW (summer)	285–500	Max	2.04	34.72	0.1	5.7	0.3	38.3	4.0	6.1
		Min	0.19	34.32	0.0	3.9	0.0	12.6	0.1	0.0
		Mean	1.40	34.65	0.0	4.2	0.1	30.2	1.0	0.4
		s.e.	0.09	0.02	0.005	0.07	0.01	1.5	0.20	0.26

Abbreviations: CDW, circumpolar deep water; LAASW, lower Antarctic surface water (winter); ND, not determined; UAASW, upper Antarctic surface water (winter); WW, winter water.

Environmental conditions encountered on the Antarctic continental shelf west of the Antarctic Peninsula on 17–24 September 2010 (LMG 10-06) and 7–30 January 2011 (LMG 11-01). See Supplementary Table 1 for the complete data set. Values shown are maximum (Max); minimum (Min); mean and standard error of the mean (s.e.) for each variable.

Betaproteobacteria *amoA* was <2% of the abundance of Archaea *amoA* in all samples and was below the limit of detection in many samples (Supplementary Table 1). Thaumarchaeota accounted for up to 16% of prokaryotes in the AASW (mean=7%) during late winter; up to 11% (mean=1.4%) in the WW; up to 26% (mean=19%) in CDW samples during late winter; and up to 29% in CDW samples during summer (mean=14%).

The differences in the abundance of Thaumarchaeota *amoA* or *rrs* genes in AASW versus CDW during late winter were not statistically significant (Figure 1 and Table 2; Student's *t*-test;  $P=0.18$  for *amoA*,  $P=0.085$  for *rrs*). In contrast, Thaumarchaeota *amoA* and *rrs* genes were less abundant in WW (means =  $4.0\text{--}2.9 \times 10^6$  copies per liter, respectively) than in CDW (means =  $12\text{--}14 \times 10^6$  copies per liter, respectively) during summer ( $P=0.0051$  for *amoA* and  $P<0.0001$  for *rrs*, Student's *t*-test; Figure 1 and Table 2), and gene abundance in WW samples varied over a wider range (Figure 1). The ratio of archaeal *amoA* to *rrs* genes was 0.62 ( $r^2=0.31$ , 95% confidence interval = 0.42–0.87) for all water masses sampled (Figure 1 and Supplementary Table 1), slightly lower compared with the ratio of 1 expected from copy numbers of these genes in sequenced Thaumarchaeota genomes. This discrepancy was taken to indicate

the potential for thaumarchaeote heterotrophy in a previous study (Kalanetra *et al.*, 2009); however, it may also be due to consistent biases in one or both of the primer sets used in qPCR (Tolar *et al.*, 2013). The abundance of Thaumarchaeota *ureC* genes was similar to the abundance of Thaumarchaeota *amoA* and *rrs* genes (Supplementary Table 1 and Figure 2). The ratio of the abundance of *ureC* versus *rrs* genes was 0.28 ( $r^2=0.69$ , 95% confidence interval = 0.24–0.33), and we found no significant differences in the ratio by water mass or season.

NMDS based on qPCR-estimated gene abundances measured in samples from the summer cruise grouped samples by water mass with CDW samples clustering tightly, driven by abundances of Thaumarchaeota (*rrs*, *amoA* and *ureC*) and *Nitrospina* (*rrs*) genes, whereas grouping of WW samples was driven by increased Bacteria *rrs* and diatom 18S rRNA gene abundances (Supplementary Figure 3b). Similar water mass-associated groupings were observed in PCA and NMDS analyses of data from the late winter cruise (Supplementary Figures 4a and b), except that increased AO rates corresponded to the AASW.

Thaumarchaeota *amoA* transcripts were more abundant in AASW than in CDW samples during late winter (means  $\pm$  s.e.:  $2.4 \pm 0.69$  versus  $0.13 \pm 0.048 \times 10^6$

**Table 2** Summary of ammonia oxidation rates, Thaumarchaeota abundance and the contribution of ammonia oxidation to bacterioplankton production on the Antarctic continental shelf

	Water mass		
	AASW (0–150 m)	WW (50–150 m)	CDW (> 150 m)
<i>Mean AO rates<sup>a</sup> (nM per day)</i>			
Late Winter (17–24 Sept 2010)	62 ± 16		21 ± 5.7
Summer (7–30 Jan 2011)		13 ± 2.8	24 ± 6.6
<i>Cells produced<sup>b</sup> (10<sup>6</sup> cells per liter per day)</i>			
Winter	3.1 ± 0.82		1.1 ± 0.28
Summer		0.66 ± 0.14	1.2 ± 0.33
<i>Biomass produced<sup>c</sup> (10<sup>6</sup> cells per liter per day)</i>			
Winter	2.3 ± 0.60		0.79 ± 0.21
Summer		0.50 ± 0.10	0.90 ± 0.25
<i>Mean abundance<sup>d</sup> (10<sup>6</sup> cells per liter)</i>			
Winter			
Archaea <i>amoA</i>	1.2 ± 0.17		0.78 ± 0.21
Thaum <i>rrs</i>	5.6 ± 0.90		2.9 ± 0.94
Summer			
Archaea <i>amoA</i>		4.0 ± 1.0	12 ± 2.7
Thaum <i>rrs</i>		2.9 ± 0.78	14 ± 1.7
<i>Specific growth rate<sup>e</sup> (per day)</i>			
Winter			
Archaea <i>amoA</i>	1.2 ± 0.21		0.85 ± 0.21
Thaum <i>rrs</i>	0.46 ± 0.11		0.45 ± 0.17
Summer			
Archaea <i>amoA</i>		0.37 ± 0.12	0.16 ± 0.04
Thaum <i>rrs</i>		0.39 ± 0.10	0.12 ± 0.03
<i>Specific nitrification rate<sup>f</sup>, λ<sub>nitrif</sub> (per day)</i>			
Winter	0.078 ± 0.015		0.026 ± 0.007
Summer		0.009 ± 0.002	0.057 ± 0.016
<i>Ammonium pool turnover time<sup>g</sup> (days)</i>			
Winter	30 ± 11		95 ± 54
Summer		608 ± 189	109 ± 30

Abbreviations: AASW, Antarctic surface water; AO, ammonia oxidation; CDW, circumpolar deep water; WW, winter water.

Means and s.e.m. are calculated using data from Supplementary Table 1.

<sup>a</sup>Average ammonia oxidation rates from this paper (Supplementary Table 1).

<sup>b</sup>Means from Supplementary Table 1, calculated assuming  $49.5 \times 10^{12}$  cells produced per mole of  $\text{NH}_4^+$  oxidized (average calculated from Figures 3 and 1 in Konneke *et al.* (2005) and Martens-Habben *et al.* (2009), respectively).

<sup>c</sup>Means from Supplementary Table 1 calculated from cells produced assuming 9 fg C per cell (Berg *et al.*, 2015).

<sup>d</sup>Calculated from average gene abundances from this paper (Supplementary Table 1) assuming *amoA* and *rrs* are single-copy genes.

<sup>e</sup>Means from Supplementary Table 1, calculated from cells produced and abundance assuming exponential growth kinetics.

<sup>f</sup>Means from Supplementary Table 1.

copies per liter, respectively;  $P=0.035$ ), but there was no significant difference in the abundance of *amoA* transcripts between the lower AASW and WW ( $3.1 \pm 1.2$  versus  $4.7 \pm 1.4 \times 10^6$  copies per liter;  $P=0.63$ ; Supplementary Table 1 and Figure 3). The abundance of *amoA* transcripts in CDW samples was not significantly different between late winter versus summer ( $0.13 \pm 0.048$  versus  $2.7 \pm 0.72 \times 10^6$  copies per liter;  $P=0.096$ ). The ratio of *amoA* transcripts per *amoA* gene was  $2.8 \pm 1.0$  for AASW versus  $0.16 \pm 0.07$  for late winter CDW ( $P=0.089$ ), and  $4.4 \pm 2.3$  for WW versus  $0.42 \pm 0.13$  for summer CDW samples ( $P=0.11$ ). Betaproteobacteria *amoA* transcript abundance was 3% (average for all samples) of Archaeal *amoA* transcript abundance, and was below the limit of detection in many samples (Supplementary Table 1).

The AO rates we measured only correlated significantly with indicators of Thaumarchaeota abundance (*rrs* and *amoA* genes), and only for samples collected during summer (all summer samples and the subset of WW samples; Figure 4 and Table 3). These correlations only explained a small portion of the variance in the AO rates ( $R$ -values ranged from 0.36 to 0.57). We found no statistically significant correlations between AO rates and either *amoA* transcript abundance or the ratio of *amoA* transcripts to genes (Figure 4 and Table 3). We found no statistically significant correlations between AO rates and Betaproteobacteria *amoA* gene abundances. *Nitrospina rrs* abundance was significantly correlated with AO rates in both WW and CDW samples during summer ( $R=0.52$ ,  $P=0.0076$ ;  $R=0.42$ ,  $P=0.05$ ; respectively).

*Thaumarchaeota* community composition

A total of 399 389 (*rrs*; mean length = 353 bp) and 154 037 (*amoA*; mean length = 358 bp) useful sequences were retained after processing (Supplementary Table 1). OTUs were defined as 97% and 98% sequence identity for *amoA* and *rrs* sequences, respectively. Thaumarchaeota populations, especially those in AASW and

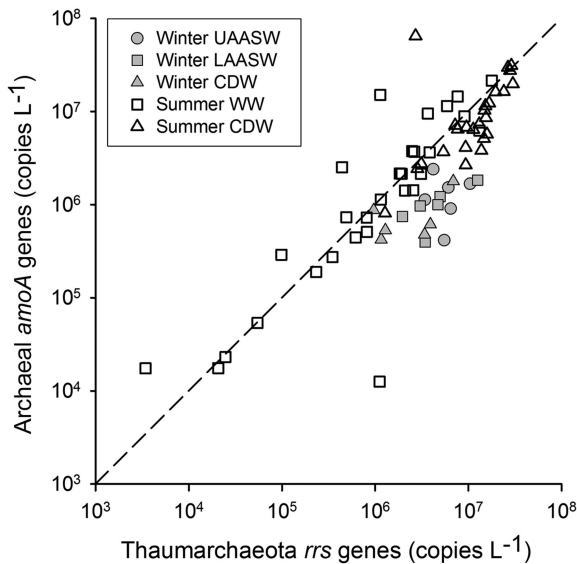


**Figure 1** Abundance of Thaumarchaeota *amoA* versus *rrs* genes in samples from Antarctic continental shelf waters. Symbols represent water masses and dates sampled as shown in the legend. Late winter samples (filled symbols) were collected in September 2010. Summer samples (open symbols) were collected in January 2011. Upper Antarctic surface water (UAASW, filled circles); lower AASW (LAASW, filled squares); and CDW (filled triangles); WW (squares); and CDW (triangles). A line of slope = 1 is shown for reference.

WW samples, were strongly dominated by a few clades (Figure 5 and Supplementary Figure 5). The CDW populations of both genes were richer than populations from AASW and WW (Supplementary Figures 6a and b). AASW and WW samples contained the same OTUs (Supplementary Figures 6c and d), with no significant difference in the composition of the populations of *rrs* or *amoA* sequences they contain (analysis of molecular variance;  $P=0.67$  and  $0.59$ , respectively). Our analysis revealed that 85% of *amoA* sequences retrieved from AASW and WW samples fell into one OTU (Figure 5). Most Thaumarchaeota *rrs* (99.8%) and *amoA* (99.1%) sequences were common to both late winter and summer CDW populations (Supplementary Figures 6e and f, the distribution of sequences among OTUs is not uniform). However, Thaumarchaeota populations differed significantly between WW and summer CDW samples (as assessed by both *rrs* and *amoA* sequences; analysis of molecular variance;  $P \leq 0.001$ ). In summary, WAP Thaumarchaeota populations were strongly differentiated by water mass (AASW or WW versus CDW), but composition within a water mass did not change through time (AASW versus WW, or late winter CDW versus summer CDW), and AASW and WW populations were strongly dominated by one OTU.

NMDS analysis of Thaumarchaeota community composition determined using high-throughput sequencing data also separated WW versus CDW samples (Supplementary Figure 7). Regressions of: AO rates ( $r^2 = 0.14$ ,  $P = 0.046$ ); AOA *amoA* transcript abundance ( $r^2 = 0.34$ ,  $P < 0.001$ ); the ratio of AOA *amoA* transcripts to genes ( $r^2 = 0.15$ ,  $P = 0.039$ ); or *Nitrospina rrs* abundance ( $r^2 = 0.18$ ,  $P = 0.024$ ) against values for *rrs* OTU positions on the primary NMDS axis (NMDS1) were

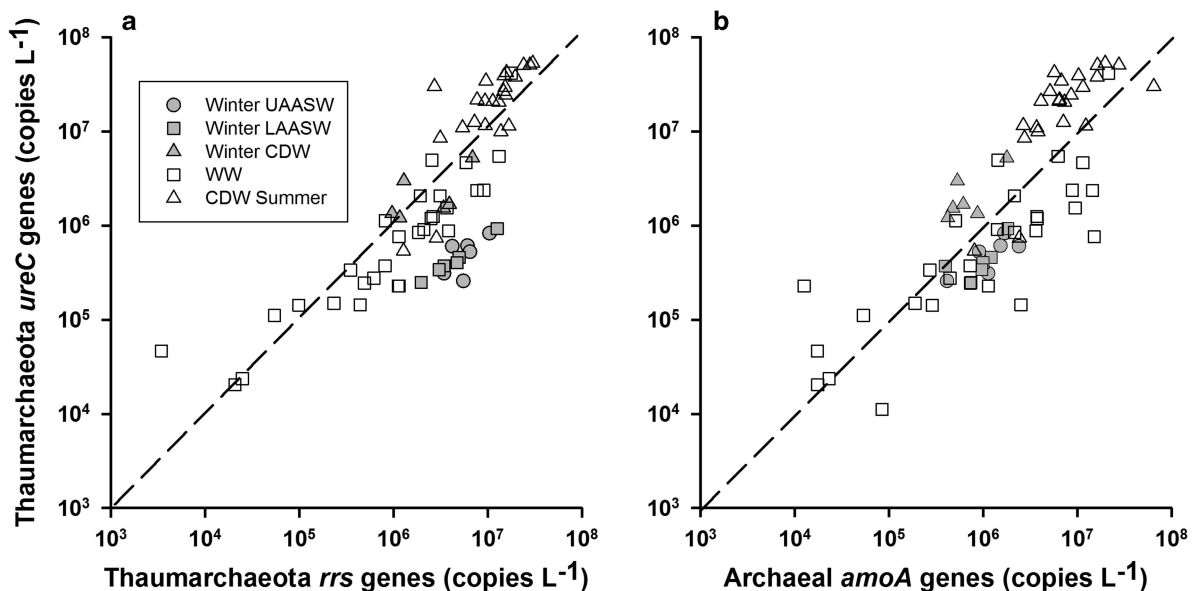


**Figure 2** Abundance of Thaumarchaeota *ureC* genes in samples from Antarctic continental shelf waters compared with the abundance of (a) archaeal *amoA* and (b) Thaumarchaeota *rrs* genes in the same sample. Symbols represent water masses and dates sampled as in Figure 1. Lines of slope = 1 are shown for reference.

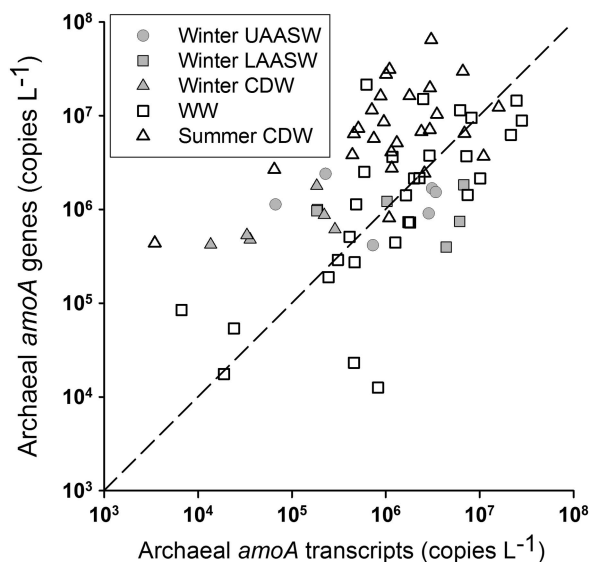


**Figure 3** Abundance of Archaea *amoA* genes versus Archaea *amoA* transcripts in samples from Antarctic coastal waters. Symbols represent water masses and dates sampled as in Figure 1. A line of slope = 1 is shown for reference.

significant. There were no statistically significant correlations between any of these variables and *amoA* OTU positions on the primary NMDS axis (NMDS1).

We found that *Nitrospina rrs* abundance covaried with Thaumarchaeota gene abundance, in agreement with distributions reported for the Pacific Ocean (Mincer et al., 2007). We also observed correlations between *Nitrospina rrs* abundance and AO rates, suggesting a tight coupling between nitrite production by AO and its oxidation by nitrite-oxidizing Bacteria in this region.

## Discussion

### Distribution of polar Thaumarchaeota

Archaeal *amoA* and *rrs* sequences retrieved from the PAL-LTER region in 2010–2011 clustered with sequences obtained from the same area in 2005–2006 by Kalanetra et al. (2009) and the phylotypes had similar distributions by water mass in both studies (Supplementary Table 4). Almost all of the WW and AASW *amoA* sequences (94% and 98%, respectively) from both studies fell into one cluster containing representative ‘near-surface clade’ clade A (Francis et al., 2005) sequences (subcluster 13; Figure 5). This clade was also dominant in libraries constructed from central Arctic Ocean samples (Kalanetra et al., 2009) and a closely related clade dominated surface samples from the Amundsen Sea (Alonso-Sáez et al., 2011). Thaumarchaeota diversity was greater in the CDW (Figure 5 and Supplementary Figures 5 and 6), consistent with previous studies of Antarctic coastal waters (Murray et al., 1998; Kalanetra et al., 2009; Alonso-Sáez et al., 2011). The strong grouping of Thaumarchaeota phylotypes by depth, and significantly lower diversity in near-surface versus

deep water samples, has been observed in other marine locations that are quite distinct from the Antarctic; for genes other than *amoA*: *rrs*, *acca* and *ureC* (Yakimov et al., 2009, 2011; Hu et al., 2011; Tolar et al., 2013); and the distinction between near-surface and deep water clades appears to be a genomic characteristic (Luo et al., 2014).

Seasonal shifts in the relative abundance of Thaumarchaeota in surface waters of polar regions have been noted previously (Murray et al., 1998; Church et al., 2003; Alonso-Sáez et al., 2008; Christman et al., 2011; Luria et al., 2014), with higher abundances in winter compared with summer. AO rates in AASW versus WW decreased from late winter to summer, with no corresponding change in AO rates in the deeper CDW. This was surprising because we expected CDW populations to respond to enhanced export of organic matter accompanying melting pack ice and the spring phytoplankton bloom (Karl et al., 1991; Ducklow et al., 2008).

### Ammonia oxidation

Our data indicate that AOB are much less abundant than AOA (Betaproteobacterial AOB *amoA* genes and transcripts were <3% of Archaeal *amoA* genes and transcripts in our samples) and we found no correlation between AO rates and the abundance of Betaproteobacterial AOB *amoA* genes or transcripts, whereas AO rates were significantly correlated with AOA *amoA* gene abundance in the same samples. AO rates per AOA cell (Supplementary Table 1) are  $14 \pm 3.4$  for the late winter cruise and  $5.6 \pm 1.2$  fmol per ammonia-oxidizer cell per day for the summer cruise. These are in the range of ammonia oxidation rates for Thaumarchaeota isolates reported in Qin et al. (2014): 2.9–12.7 fmol per ammonia-oxidizer cell per day. Although we cannot definitively exclude the possibility of a significant contribution by Betaproteobacterial AOB to the AO rates we measured, our analysis does not suggest excess AO that needs to be accounted for by something other than the Thaumarchaeota we detected in our samples.

There are no other comparable AO rate measurements from Antarctic coastal waters, and only a handful of observations from the Southern Ocean. Bianchi et al. (1997) reported AO rates of 25.6 nM per day (averaged over depths 0–100 m) at their southernmost station in the Indian Ocean (52°S, 62°E; north of the Polar Front) during the fall. Olson (1981b) measured AO rates that averaged 2.8 nM per day ( $n = 23$ , range 0–13 nM per day) in open ocean waters south of the Polar Front in the Scotia Sea (25°W to 60°W and 55°S to 61°S), from depths <100 m, during late winter. These rates are more than an order of magnitude lower compared with the rates we measured in late winter ( $62 \pm 16$ ; Table 2). Olson (1981a) also measured AO rates in two samples retrieved from 30 and 300 m in the Ross Sea during summer. These rates (6.0 and 8.9 nM per day, respectively) are also lower compared with our summer measurements



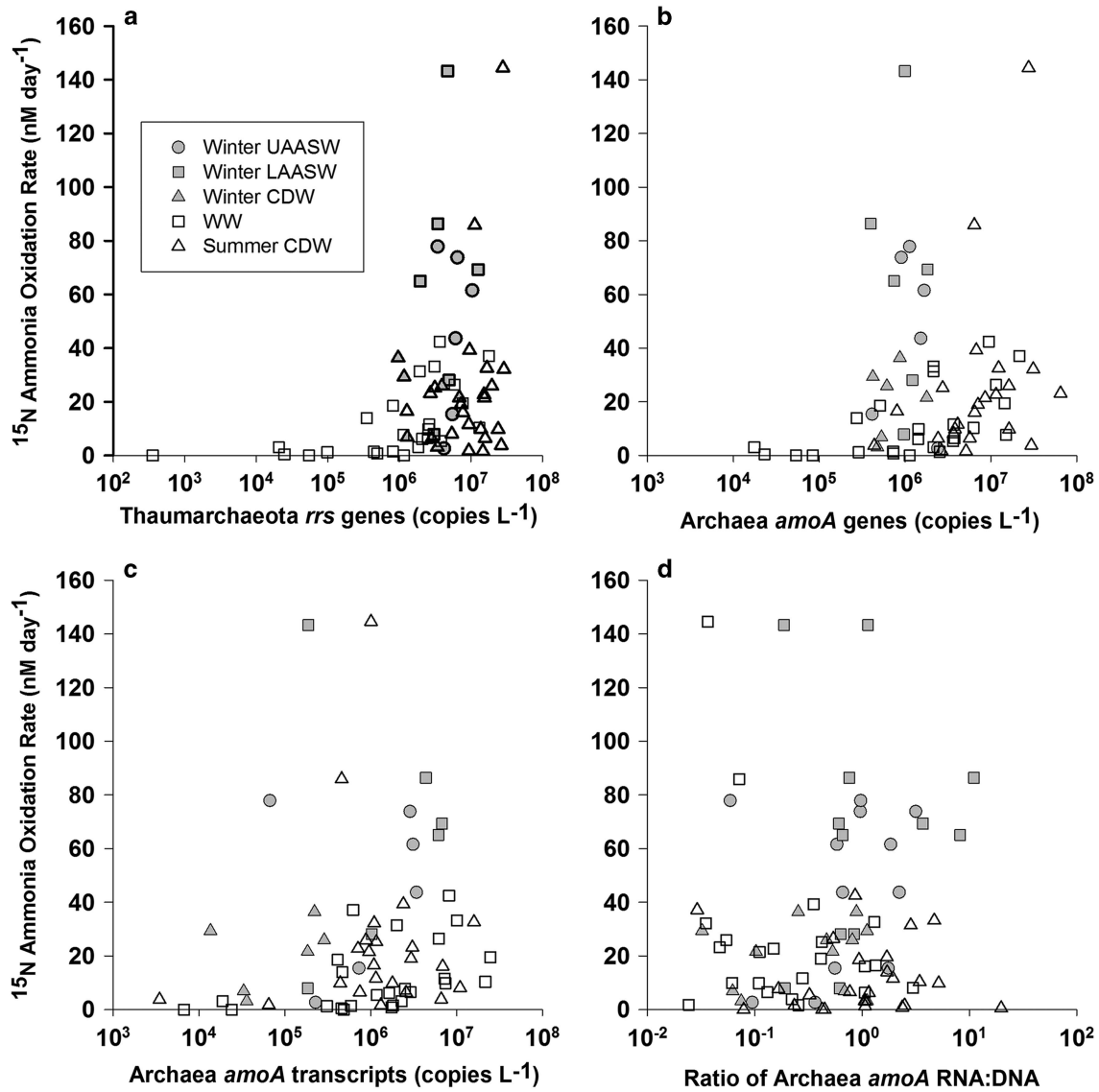


**Figure 4** Relationship between AO rate and gene and transcript abundance. Panels show AO rates plotted against: (a) archaeal *rrs* gene abundance; (b) archaeal *amoA* gene abundance; (c) archaeal *amoA* transcript abundance; and (d) the ratio of archaeal *amoA* transcripts to genes (mRNA/DNA). Symbols represent water masses and dates sampled as in Figure 1.

**Table 3** Correlations (*r*) between ammonia oxidation rates and Thaumarchaeota gene or transcript abundance, measured in Antarctic coastal waters

Sample subset	n	<i>rrs genes</i>	<i>amoA genes</i>	<i>amoA transcripts</i>	Ratio of <i>amoA mRNA:DNA</i>
All winter	18	+0.25	-0.009	+0.41	+0.40
UAASW	6	+0.24	-0.30	-0.38	+0.30
LAASW	6	+0.099	-0.14	+0.082	+0.17
CDW	6	-0.15	+0.21	+0.56	+0.44
All summer	47	+0.45***	+0.36*	+0.025	-0.16
WW	25	+0.52***	+0.57**	+0.33	-0.13
CDW	22	+0.33	+0.23	-0.11	-0.21

Abbreviations: CDW, circumpolar deep water; LAASW, lower Antarctic surface water; UAASW, upper Antarctic surface water; WW, winter water. Statistically significant correlations are indicated as follows: \*\*\* $P < 0.001$ , \*\* $P < 0.01$  and \* $P < 0.05$ .

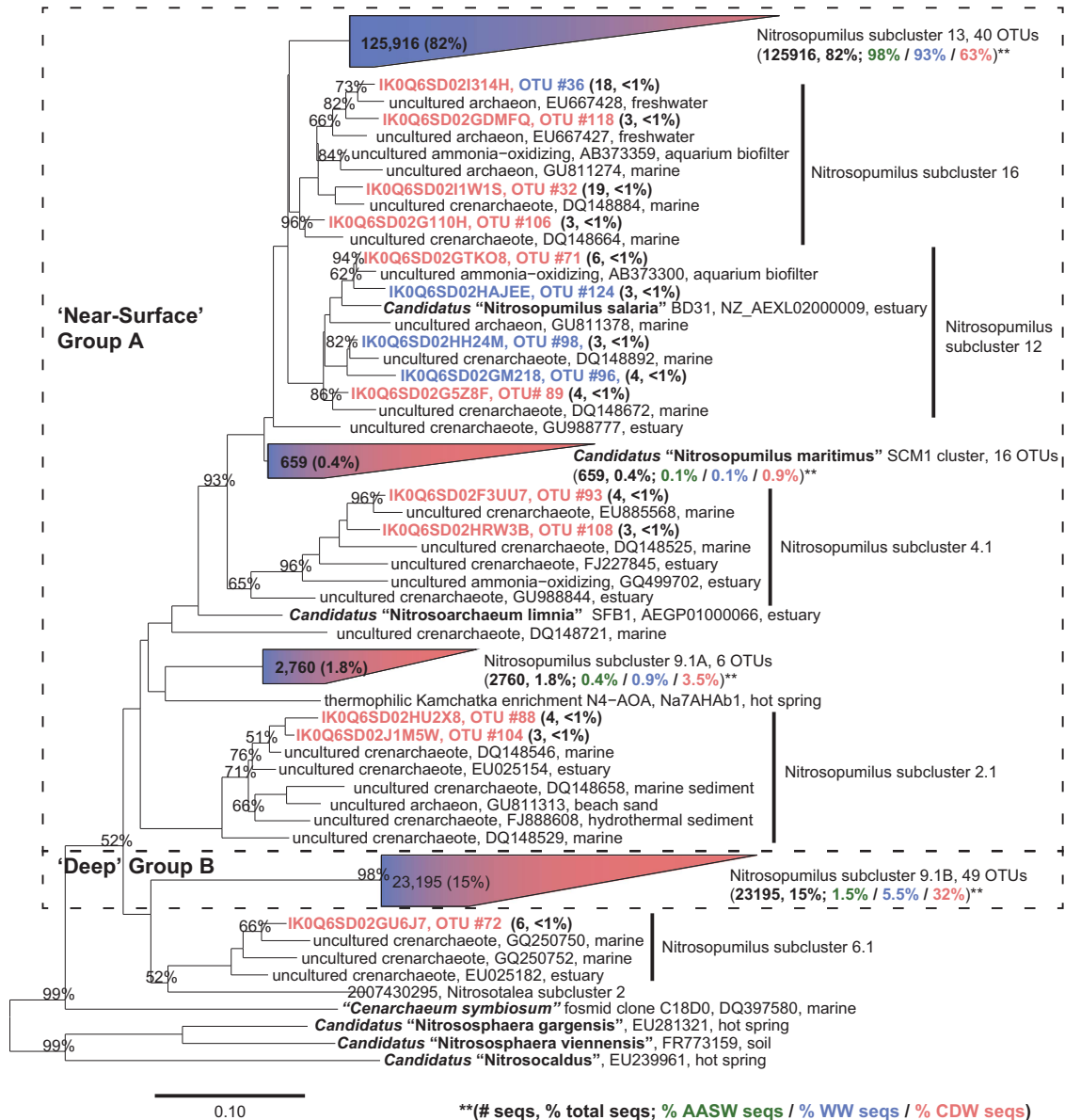


**Figure 5** Phylogenetic analysis of Archaea *amoA* sequences retrieved from the study area. Partial sequences (359 bp) of Thaumarchaeota *amoA* genes obtained by high-throughput sequencing were aligned against the Pester *et al.* (2012) database and the neighbor-joining tree was constructed in ARB. OTUs were defined at 97% similarity. Numbers following each OTU give the number of sequences and % of total sequences it represents. Additional notations apply to four major clades to indicate the % of sequences in these clades from each water mass sampled (AASW—green; WW—blue; CDW—red). Shading of trapezoids representing sequences assigned to four major clades indicates the relative contribution of sequences from AASW+WW (blue) versus all CDW (red) to these clades. Dashed boxes delineate archaeal *amoA* groups A (surface water) and B (deep water) as defined in Francis *et al.* (2005). Only bootstrap values  $\geq 50\%$  (of 1000 iterations) are shown.

(mean = 18 nM per day). It seems unlikely that the differences in analytical methods used by Olson (Wada and Hattori, 1972; Schell, 1978) versus our study would lead to a systematic bias that could account for the differences in rates.

AO rates in our samples (overall mean = 27 nM per day) were also higher than potential rates (added  $^{15}\text{NH}_4\text{Cl} = 1 \mu\text{M}$ ) measured in shallow water (2 m), nearshore Arctic communities, which ranged from 3.6 nM per day (winter mean of four samples) to 0.14 nM per day (summer mean of four samples; Christman *et al.*, 2011). The abundance of Archaea in

the Arctic samples (Christman *et al.*, 2011) was much lower compared with that we found in Antarctic coastal waters (means of 0.008% and 1.2% of prokaryotes for summer and winter samples, respectively), consistent with a previous comparison (Kalanetra *et al.*, 2009).

*Correlation of rates with gene and transcript abundance*  
It is of interest to know whether AO rates can be predicted from measurements of gene or transcript abundance (or ratios), because it is typically easier

and faster to measure gene or transcript abundance than AO rates. We only found significant ( $P < 0.05$ ) correlations between AO rates and Thaumarchaeota gene abundance for selected subsets of our data: WW, or all summer samples (Table 3). We did not find a relationship between transcript abundance and rates. Although we processed mRNA samples as rapidly as possible after the water sample was available to us, the lack of a correlation might be a result of rapid changes in the mRNA content of Thaumarchaeota (Feike *et al.*, 2011) as a consequence of changes that take place during the time required for processing samples (Moran *et al.*, 2013). Alternatively, transcription and AO activity may not be tightly coupled in these populations. Activity requires translation of the mRNA into a protein, the nascent protein may require further processing, including the insertion of cofactors, and AO may be tied more closely to the activity of proteins other than *amoA*. Thus, lack of a significant correlation between *amoA* transcript abundance and AO is not surprising. Santoro *et al.* (2010) found no correlation between AO rates and *amoA* abundance for samples from the central California Current. They postulated that this might be due to differences in cell-specific AO rates among Thaumarchaeota ecotypes. This was shown in studies of Monterey Bay by Smith *et al.* (2014), who found significant correlations between AO rates and the abundance of *amoA* genes from the 'surface water' clade (WCA) of Thaumarchaeota, but not with the 'deep water' clade (WCB) or with total *amoA* gene abundance. This depth distribution of ecotypes is similar to the difference we noted between WW and CDW samples on the summer cruise. Although there seems to be a weak relationship between AO and gene abundance in some sets of samples (this study; Beman *et al.*, 2008), the inconsistency of this relationship cautions against trying to predict AO rates from *amoA* gene or transcript abundance or ratios.

#### Geochemical consequences

The rates we measured in the Antarctic are comparable to rates measured in an upwelling zone off Monterey Bay: 0–210 nM per day, with a mean of ~100 nM per day (Santoro *et al.*, 2010), or 0–70 nM per day, with a mean of ~20 nM per day (Smith *et al.*, 2014); and in an oceanic oxygen minimum zone: 0–348 nM per day, with a mean of ~50 nM per day (Beman *et al.*, 2012, 2013). Taking the area of oceanic oxygen minimum zones (8% of the global ocean; Paulmier and Ruiz-Pino, 2009) as a proxy for the area of elevated nitrification rates and assuming no nitrification in the rest of the ocean, the contribution of nitrification on the Antarctic continental shelf to the global oceanic total would be ~9% (Supplementary Table 5). Although rough, these calculations serve to demonstrate the potential importance of nitrification in Antarctic coastal waters to the global nitrogen cycle.

Yool *et al.* (2007), who were interested in the impact of AO on new production measurements

(Dugdale and Goering, 1967; Eppley and Peterson, 1979), reported that specific nitrification rates ( $\lambda_{\text{nitrif}}$ , calculated by dividing the AO rate by the concentration of ammonia in a sample), ranged from 0.001 to 10 per day (mean = 0.55 per day) across the global ocean, with Olson's Antarctic samples (Olson 1981a, b) an order of magnitude lower, on average (mean = 0.017 per day).  $\lambda_{\text{nitrif}}$  values calculated from our data (mean for all data = 0.041 per day; range = 0.0003–0.31 per day; Supplementary Table 1) were on average 2.4 times greater than those reported by Yool *et al.* (2007) for Olson's data.

The inverse of  $\lambda_{\text{nitrif}}$  is the turnover time of the ammonium pool as a result of its oxidation to nitrite (this does not include ammonium pool turnover driven by phytoplankton or bacterioplankton assimilation). This ranged from 5.2 to 3400 days with a mean of 269 days for our samples (Supplementary Table 1). There were no statistically significant differences in ammonium pool turnover times between AASW, spring CDW and summer CDW samples (Table 2); however, turnover times were significantly longer in WW samples than in AASW (608 versus 30 days,  $P = 0.032$ ) or summer CDW samples (608 versus 109 days,  $P = 0.013$ ).

Nitrate-based phytoplankton growth supplies labile organic nitrogen that can be regenerated rapidly via zooplankton grazing and the microbial loop (Azam *et al.*, 1983) to replenishing ammonium consumed by AO. However, phytoplankton growth, and thus nitrate assimilation, is greatly reduced during the polar winter, decreasing the flux of ammonium from this source. The mean turnover time of the AASW ammonia pool as a result of AO (30 days; Table 1) is shorter than the duration of the Antarctic winter, indicating the need for an alternate source of ammonium, presumably excretion by eukaryotes or metazoa or the slow degradation of moderately labile organic nitrogen (Manganelli *et al.*, 2009), to support winter chemoautotrophy based on AO. The AO rates we measured were higher in winter compared with summer, despite the inferred decrease in ammonia regeneration flux in winter versus summer. This suggests that inhibition (e.g., Murray *et al.*, 1998) may be more important than ammonium supply in controlling thaumarchaeote production during summer.

#### Contribution of AO to chemoautotrophy and bacterioplankton productivity

Chemoautotrophic carbon fixation by Thaumarchaeota cells was estimated from AO rates (Supplementary Table 1) using 10 mol of ammonium oxidized to nitrite per mole of C fixed (Berg *et al.*, 2015). We also estimated the production of new thaumarchaeote cells and Thaumarchaeota biomass from the relationships between ammonium consumed and Nitrosopumilus cells produced from Figure 3 in Konneke *et al.* (2005) and Figure 1 in Martens-Habbena *et al.* (2009): 46.6 and 52.4 (mean = 49.5) cells per nmol ammonium oxidized, respectively. Our estimates ranged from

0.05 to 22 nM of C fixed per liter per day and  $0.026\text{--}10.9 \times 10^6$  cells per liter per day. When combined with estimates of Thaumarchaeota abundance (from *amoA* or *rrs* abundance), population growth rates averaged 0.50 per day (all *amoA* data, range 0.01–2.5 per day) or 0.31 per day (all *rrs* data, range 0.01 to 2.1 per day). Growth rates differed among water masses (analysis of variance  $P=0.001$  for rates calculated using *amoA*,  $P=0.013$  for rates calculated using *rrs*), with higher growth rates during late winter than summer (all depths: *amoA* means 1.1 versus 0.26 per day,  $P<0.0001$ ; *rrs* means 0.45 versus 0.25 per day,  $P=0.092$ ). Calculated growth rates were higher in AASW and WW versus CDW (Table 2), although only the summer comparison based on *rrs* gene abundance was statistically significant:  $0.39 \pm 0.10$  versus  $0.12 \pm 0.03$ ,  $P=0.016$ .

Taking the rates we measured during late winter to represent those of fall and winter, and integrating over a mean continental shelf water column depth of 475 m, the mean area-specific rates we measured are equivalent to 10.1 and 14.7 mmol of ammonium-N oxidized per m<sup>2</sup> per day in summer versus fall+winter+spring, respectively (Supplementary Table 6a). Chemoautotrophic carbon fixation supported by ammonium oxidation can be calculated to be 0.5 mol C per m<sup>2</sup> per year; or about 3% of the annual average photoautotrophic primary production of 15 mol C per m<sup>2</sup> per year estimated for the Antarctic continental shelf by Arrigo *et al.* (1998) (Supplementary Table 6b), or 5.7% of an average of 8.1 mol C per m<sup>2</sup> per year (range 0.4–16.3%; Supplementary Table 6c) estimated for the PAL-LTER study area (from Ducklow *et al.*, 2012).

Chemoautotrophy has been proposed as a means of maintaining bacterioplankton productivity, and thus the microbial food web, during the Antarctic winter (Manganelli *et al.*, 2009; Grzymalski *et al.*, 2012). We estimate that production of biomass supported by AO is 1.5 g C per m<sup>2</sup> over the 8 months of fall, winter and spring (Supplementary Table 6a). This production is consistent with estimates based on incorporation of L-leucine and dissolved inorganic carbon reported by Manganelli *et al.* (2009). They concluded that chemoautotrophic production could account for 20% of winter bacterioplankton production, or about 3.5 g C per m<sup>2</sup> when integrated over the same depth range we used (see Supplementary Table 6d) in waters of the southern Drake Passage. Our calculations suggest that production of ammonia oxidizer biomass could account for about 8.8% of winter bacterioplankton production at this site.

Annual integrated bacterioplankton production in the Ross Sea is about 23 g C per m<sup>2</sup> per year (Supplementary Table 6e, calculated from Ducklow *et al.*, 2001), but this includes elevated rates in summer coupled to phytoplankton production. Our estimates suggest that production of ammonia oxidizer biomass could account for about 9% of this annually integrated total. The winter rates of bacterioplankton production they measured (0.8 mmol C per m<sup>2</sup> per day) are comparable to the rates we estimate from AO

(0.5 mmol C per m<sup>2</sup> per day), as are winter rates of bacterioplankton production referenced in Grzymalski *et al.* (2012). Assuming that Thaumarchaeota take up and incorporate exogenous L-leucine, a significant portion of the winter bacterioplankton production measured on the WAP shelf may be growth of the Thaumarchaeota population, as proposed by Grzymalski *et al.* (2012). Alternatively, if Thaumarchaeota do not incorporate L-leucine to the same extent as Bacteria (i.e., data presented in Alonso-Sáez *et al.*, 2008), then production supported by AO may be in addition to heterotrophic production measured by L-leucine incorporation. In either case, our data indicate that Thaumarchaeota can account for a significant portion of prokaryotic production during the Antarctic winter.

Thaumarchaeota production is unlikely to be able to meet all of the energy demand, because heterotrophic decomposition of organic matter is required to supply the ammonium to be oxidized. Assuming Redfield stoichiometry for labile organic matter (Redfield *et al.*, 1963) and that ammonium release is linked to complete oxidation of that organic matter, 6.6 mol of C must be mineralized per mole of ammonium regenerated. For each mole of Thaumarchaeota biomass C produced, ~27 mol of ammonia are oxidized by Thaumarchaeota; thus, 178 mol of labile organic C must be oxidized to support chemoautotrophic production of 1 mol of Thaumarchaeota C, unless AOA are mixotrophic or heterotrophic (Spang *et al.*, 2012; Qin *et al.*, 2014; Lin *et al.*, 2015) or they are able to access other forms of reduced nitrogen (e.g., organic nitrogen in urea or other small molecules) more directly. Note that chemoautotrophy fueled by AO is not 'new production', *sensu* Eppley and Peterson (1979), even though carbon is being fixed: since AO depends on a source of reduced N supplied by organic matter mineralization, at an ecosystem level it is part of a net oxidative process (Smith and Hollibaugh, 1989).

## Conclusions

AO rates measured in Antarctic continental shelf waters ranged from <0.1 to 220 nM per day and are an order of magnitude greater than rates previously reported for other Southern Ocean waters (Scotia Sea, Ross Sea). AOA populations in the surface mixed layer during winter oxidize ammonia at higher rates than those in the summer 'WW' layer that is derived from the winter mixed layer. AO rates in CDW samples have not been measured previously. They are comparable to rates measured by others in temperate waters, suggesting that the contribution of the Southern Ocean to global nitrification has been underestimated. Chemoautotrophic production supported by AO can account for a ~9% of winter bacterioplankton production in the study area, but must be supported by ongoing ammonium regeneration. *amoA* transcript abundance was 0.02–40% of *amoA* gene abundance across all water masses. Despite this large dynamic range, we only found significant correlations between

AO rates and gene abundance, and only for a selected subset of our samples. This suggests caution in using *amoA* transcript abundance or transcript to gene ratios to predict AO rates in the environment.

## Conflict of Interest

The authors declare no conflict of interest.

## Acknowledgements

We thank the officers and crew of the ARSV *Laurence M Gould* and staff of Raytheon Polar Services Company for support during LMG 10-06 and LMG 11-01, especially E Pohlman, D Morehouse, S Alesandrini, T Baldwin and J Miller. We appreciate the assistance of R Jellison and the Palmer Station 2010–2011 Summer Crew with sample collection, and also thank L Ekern, S Moret and C Guest for technical and scientific expertise on the LMG, and H Ducklow and the Palmer LTER (funded through Grant ANT 08-23101) for additional support for LMG 11-01. Additionally, we thank J Wagner, C Givens, C Edwardson, C Ka'apu-Lyons, A Bratcher, L Lim, D Di Iorio and S Holland for assistance with analyses. GIS analyses that provided metrics of Antarctic coastal waters were provided by G Roth at the Polar Geospatial Center, University of Minnesota. This manuscript benefited from thoughtful comments by anonymous reviewers of a previous draft. This work was supported by the US National Science Foundation through Grants ANT 08-38996, OCE 09-43278 (both to JTH); and OCE 11-29260 (to BNP), and by the University of Georgia Graduate School (2011 Innovative and Interdisciplinary Research Grant to BBT). This is SOEST contribution number 9571.

## Author contributions

JTH and BBT designed the research; JTH, BBT and LIA conducted the sampling program; BBT, JTH, MJR, NJW, QL and BNP contributed to sample analysis; BBT, JTH and BNP analyzed the data; BBT and JTH wrote the paper with input from the coauthors.

## References

Alonso-Sáez L, Andersson A, Heinrich F, Bertilsson S. (2011). High archaeal diversity in Antarctic circumpolar deep waters. *Environ Microbiol Rep* **3**: 689–697.

Alonso-Sáez L, Sánchez O, Gasol JM, Balagué V, Pedrós-Alio C. (2008). Winter-to-summer changes in the composition and single-cell activity of near-surface Arctic prokaryotes. *Environ Microbiol* **10**: 2444–2454.

Alonso-Sáez L, Waller AS, Mende DR, Bakker K, Farnelid H, Yager PL *et al.* (2012). Role for urea in nitrification by polar marine Archaea. *Proc Natl Acad Sci USA* **109**: 17989–17994.

Arrigo KR, Worthen D, Schnell A, Lizotte MP. (1998). Primary production in Southern Ocean waters. *J Geophys Res* **103**: 15587–15600.

Azam F, Fenchel T, Field JG, Gray JS, Meyer-Riel LA, Thingstad F. (1983). Ecological role of water column microbes in the sea. *Mar Ecol Progr Ser* **10**: 257–263.

Azam F, Smith DC, Hollibaugh JT. (1991). The role of the microbial loop in Antarctic pelagic ecosystems. In: Sakshaug E, Hopkins CCE, Oritsland NA (eds). *Proceedings of the Pro Mare Symposium on Polar Marine Ecology Trondheim*, vol. 10, Norway 12–16 May 1990, pp 239–243.

Baldi F, Facca C, Marchetto D, Nguyen TNM, Spurio R. (2011). Diatom quantification and their distribution with salinity brines in coastal sediments of Terra Nova Bay (Antarctica). *Mar Environ Res* **71**: 304–311.

Bano N, Hollibaugh JT. (2000). Diversity and distribution of DNA sequences with affinity to ammonia-oxidizing bacteria of the  $\beta$ -subdivision of the Class Proteobacteria in the Arctic Ocean. *Appl Environ Microbiol* **66**: 1960–1969.

Beman JM, Chow C-E, King AL, Feng Y, Fuhrman JA, Andersson A *et al.* (2011). Global declines in oceanic nitrification rates as a consequence of ocean acidification. *Proc Natl Acad Sci USA* **108**: 208–213.

Beman JM, Leilei Shih J, Popp BN. (2013). Nitrite oxidation in the upper water column and oxygen minimum zone of the eastern tropical North Pacific Ocean. *ISME J* **7**: 2192–2205.

Beman JM, Popp BN, Alford SE. (2012). Quantification of ammonia oxidation rates and ammonia-oxidizing archaea and bacteria at high resolution in the Gulf of California and eastern tropical North Pacific Ocean. *Limnol Oceanogr* **57**: 711–726.

Beman JM, Popp BN, Francis CA. (2008). Molecular and biogeochemical evidence for ammonia oxidation by marine Crenarchaeota in the Gulf of California. *ISME J* **2**: 429–441.

Berg C, Listmann L, Vandieken V, Vogts A, Jürgens K. (2015). Chemoautotrophic growth of ammonia-oxidizing Thaumarchaeota enriched from a pelagic redox gradient in the Baltic Sea. *Front Microbiol* **5**: 786.

Bianchi M, Feliatra, Teguier P, Vincendeau MA, Morvan J. (1997). Nitrification rates, ammonium and nitrate distributions in upper layers of the water column and sediments of the Indian sector of the Southern Ocean. *Deep-Sea Res II* **44**: 1017–1032.

Biers EJ, Sun S, Howard EC. (2009). Prokaryotic genomes and diversity in the surface ocean: interrogating the Global Ocean Sampling metagenome. *Appl Environ Microbiol* **75**: 2221–2229.

Brzezinski MA, Phillips DR, Chavez FP, Friederich GE, Dugdale RC. (1997). Silica production in the Monterey, California, upwelling system. *Limnol Oceanogr* **42**: 1694–1705.

Christman GD, Cottrell MT, Popp BN, Gier E, Kirchman DL. (2011). Abundance, diversity, and activity of ammonia-oxidizing prokaryotes in the coastal Arctic Ocean in summer and winter. *Appl Environ Microbiol* **77**: 2026–2034.

Church MJ, DeLong EF, Ducklow HW, Karner MB, Preston CM, Karl DM. (2003). Abundance and distribution of planktonic Archaea and Bacteria in the waters west of the Antarctic Peninsula. *Limnol Oceanogr* **48**: 1893–1902.

Connelly TL, Baer SE, Cooper JT, Bronk DA, Wawrik B. (2014). Urea uptake and carbon fixation by marine pelagic Bacteria and Archaea during the Arctic summer and winter seasons. *Appl Environ Microbiol* **80**: 6013–6022.

- DeLong EF, Wu KY, Prezelin BB, Jovine RVM. (1994). High abundance of Archaea in Antarctic marine picoplankton. *Nature* **371**: 695–697.
- Dore JE, Popp BN, Karl DM, Sansone FJ. (1998). A large source of atmospheric nitrous oxide from subtropical North Pacific surface waters. *Nature* **396**: 63.
- Ducklow HW, Baker K, Martinson DG, Quetin LB, Ross RM, Smith RC et al. (2007). Marine pelagic ecosystems: the West Antarctic Peninsula. *Phil Trans R Soc Ser B* **362**: 67–94.
- Ducklow H, Carlson C, Church M, Kirchman D, Smith D, Steward G. (2001). The seasonal development of the bacterioplankton bloom in the Ross Sea, Antarctica, 1994–1997. *Deep-Sea Res II* **48**: 4199–4221.
- Ducklow HW, Erickson M, Kelly J, Montes-Hugo M, Ribic CA, Smith RC et al. (2008). Particle export from the upper ocean over the continental shelf of the west Antarctic Peninsula: a long-term record, 1992–2007. *Deep-Sea Res II* **55**: 2118–2131.
- Ducklow HW, Schofield O, Vernet M, Stammerjohn S, Erickson M. (2012). Multiscale control of bacterial production by phytoplankton dynamics and sea ice along the western Antarctic Peninsula: a regional and decadal investigation. *J Mar Syst* **98–99**: 26–39.
- Dugdale RC, Goering JJ. (1967). Uptake of new and regenerated forms of nitrogen in primary productivity. *Limnol Oceanogr* **12**: 196–206.
- Eppley RW, Peterson BJ. (1979). Particulate organic matter flux and planktonic new production in the deep ocean. *Nature* **282**: 677–680.
- Excoffier L, Smouse PE, Quattro JM (1992). Analysis of molecular variance inferred from metric distances among DNA haplotypes: application to human mitochondrial DNA restriction data. *Genetics* **131**: 479–491.
- Feike J, Jurgens K, Hollibaugh JT, Kruger S, Jost G, Labrenz M. (2011). Measuring unbiased metatranscriptomics in suboxic waters of the central Baltic Sea using a new in situ fixation system. *ISME J* **6**: 461–470.
- Francis CA, Roberts KJ, Beman JM, Santoro AE, Oakley BB. (2005). Ubiquity and diversity of ammonia-oxidizing Archaea in water columns and sediments of the ocean. *Proc Natl Acad Sci USA* **102**: 14683–14688.
- Gifford SM, Sharma S, Rinta-Kanto JM, Moran MA. (2011). Quantitative analysis of a deeply sequenced marine microbial metatranscriptome. *ISME J* **5**: 461–472.
- Grzymiski JJ, Riesenfeld CS, Williams TJ, Dussaq AM, Ducklow H, Erickson M et al. (2012). A metagenomic assessment of winter and summer bacterioplankton from Antarctica Peninsula coastal surface waters. *ISME J* **6**: 1901–1915.
- Hofmann EE, Klinck JM. (1998). Hydrography and circulation of the Antarctic continental shelf: 150E to the Greenwich meridian. In: Robinson AR, Brink KH (eds), *The Sea*. Wiley: New York, NY, USA, pp 997–1042.
- Hollibaugh JT, Gifford SM, Moran MA, Ross MJ, Sharma S, Tolar BB. (2014). Seasonal variation in the metatranscriptomes of a Thaumarchaeota population from SE USA coastal waters. *ISME J* **8**: 685–698.
- Hu A, Jiao N, Zhang CL. (2011). Community structure and function of planktonic Crenarchaeota: changes with depth in the South China Sea. *Microb Ecol* **62**: 549–563.
- Jones MN. (1984). Nitrate reduction by shaking with cadmium: alternative to cadmium columns. *Water Res* **18**: 643–646.
- Kalanetra KM, Bano N, Hollibaugh JT. (2009). Ammonia-oxidizing Archaea in the Arctic Ocean and Antarctic coastal waters. *Environ Microbiol* **11**: 2434–2445.
- Karl DM, Tilbrook BD, Tien G. (1991). Seasonal coupling of organic matter production and particle flux in the western Bransfield Strait, Antarctica. *Deep-Sea Res* **38**: 1097–1126.
- Konneke M, Bernhard AE, de la Torre JR, Walker CB, Waterbury JB, Stahl DA. (2005). Isolation of an autotrophic ammonia-oxidizing marine archaeon. *Nature* **437**: 543–546.
- Legendre P, Legendre L (1998). *Numerical Ecology*, 2nd English edn Amsterdam, Netherlands: Elsevier Science BV.
- Lin X, Handley KM, Gilbert JA, Kostka JE. (2015). Metabolic potential of fatty acid oxidation and anaerobic respiration by abundant members of Thaumarchaeota and Thermoplasmata in deep anoxic peat. *ISME J* **9**: 2740–2744.
- Luo H, Tolar BB, Swan BK, Zhang CL, Stepanauskas R, Ann Moran M et al. (2014). Single-cell genomics shedding light on marine Thaumarchaeota diversification. *ISME J* **8**: 732–736.
- Luria CM, Ducklow HW, Amaral-Zettler LA. (2014). Marine bacterial, archaeal and eukaryotic diversity and community structure on the continental shelf of the western Antarctic Peninsula. *Aquat Microb Ecol* **73**: 107–121.
- Manganelli M, Malfatti F, Samo TJ, Mitchell BG, Wang H, Azam F. (2009). Major role of microbes in carbon fluxes during austral winter in the southern Drake Passage. *PLoS One* **4**: e6941.
- Martens-Habbena W, Berube PM, Urakawa H, de la Torre JR, Stahl DA. (2009). Ammonia oxidation kinetics determine niche separation of nitrifying Archaea and Bacteria. *Nature* **461**: 976–979.
- Martinson DG, Stammerjohn SE, Iannuzzi RA, Smith RC, Vernet M. (2008). Western Antarctic Peninsula physical oceanography and spatio-temporal variability. *Deep Sea Res II* **55**: 1964–1987.
- Massana R, Taylor LT, Murray AE, Wu KY, Jeffrey WH, DeLong EF. (1998). Vertical distribution and temporal variation of marine planktonic archaea in the Gerlache Strait, Antarctica, during early spring. *Limnol Oceanogr* **43**: 607–617.
- Mincer TJ, Church MJ, Taylor LT, Preston C, Karl DM, DeLong EF. (2007). Quantitative distribution of presumptive archaeal and bacterial nitrifiers in Monterey Bay and the North Pacific Subtropical Gyre. *Environ Microbiol* **9**: 1162–1175.
- Moran MA, Satinsky B, Gifford SM, Luo H, Rivers A, Chan L-K et al. (2013). Sizing up metatranscriptomics. *ISME J* **7**: 237–243.
- Murray AE, Preston CM, Massana R, Taylor LT, Blakis A, Wu K et al. (1998). Seasonal and spatial variability of Bacterial and Archaeal assemblages in the coastal waters near Anvers Island, Antarctica. *Appl Environ Microbiol* **64**: 2585–2595.
- Murray AE, Wu KY, Moyer CL, Karl DM, DeLong EF. (1999). Evidence for circumpolar distribution of planktonic Archaea in the Southern Ocean. *Aquat Microb Ecol* **18**: 263–273.
- Nguyen TNM, Berzano M, Gualerzi CO, Spurio R. (2011). Development of molecular tools for the detection of freshwater diatoms. *J Microbiol Methods* **84**: 33–40.
- Olson RJ. (1981a). Differential photoinhibition of marine nitrifying bacteria: a possible mechanism for the

- formation of the primary nitrite maximum. *J Mar Res* **39**: 227–238.
- Olson RJ. (1981b). <sup>15</sup>N tracer studies of the primary nitrite maximum. *J Mar Res* **39**: 203–226.
- Paulmier A, Ruiz-Pino D. (2009). Oxygen minimum zones (OMZs) in the modern ocean. *Progr Oceanogr* **80**: 113–128.
- Pedneault E, Galand PE, Potvin M, Tremblay J-É, Lovejoy C. (2014). Archaeal *amoA* and *ureC* genes and their transcriptional activity in the Arctic Ocean. *Scientific Rep* **4**: 4661.
- Pester M, Rattei T, Flechl S, Gröngröft A, Richter A, Overmann J *et al.* (2012). *amoA*-based consensus phylogeny of ammonia-oxidizing archaea and deep sequencing of *amoA* genes from soils of four different geographic regions. *Environ Microbiol* **14**: 525–539.
- Popp BN, Sansone FJ, Rust TM, Merritt DA. (1995). Determination of concentration and carbon isotopic composition of dissolved methane in sediments and nearshore waters. *Anal Chem* **67**: 405–411.
- Poretsky RS, Bano N, Buchan A, LeClerc G, Kleikemper J, Pickering M *et al.* (2005). Analysis of microbial gene transcripts in environmental samples. *Appl Environ Microbiol* **71**: 4121–4126.
- Qin W, Amin SA, Martens-Habbena W, Walker CB, Urakawa H, Devol AH *et al.* (2014). Marine ammonia-oxidizing archaeal isolates display obligate mixotrophy and wide ecotypic variation. *Proc Natl Acad Sci USA* **111**: 12504–12509.
- Redfield AC, Ketchum BH, Richards FA. (1963). The influence of organisms on the composition of seawater. In: Hill MN (ed), *The Sea*, Vol 2. Interscience: Hoboken, NJ, USA, pp 26–77.
- Santoro AE, Casciotti KL, Francis CA. (2010). Activity, abundance and diversity of nitrifying archaea and bacteria in the central California Current. *Environ Microbiol* **12**: 1989–2006.
- Schell DW. (1978). Chemical and isotopic methods in nitrification studies. In: Schlessinger D (ed). *Microbiology*. American Society for Microbiology: Washington, DC, USA.
- Schloss PD, Gevers D, Westcott SL. (2011). Reducing the effects of PCR amplification and sequencing artifacts on 16S rRNA-based studies. *PLoS One* **6**: e27310.
- Sigman DM, Casciotti KL, Andreani M, Barford C, Galanter M, Bohlke JK. (2001). A bacterial method for the nitrogen isotopic analysis of nitrate in seawater and freshwater. *Anal Chem* **73**: 4145–4153.
- Smart SM, Fawcett SE, Thomalla SJ, Weigand MA, Reason CJC, Sigman DM. (2015). Isotopic evidence for nitrification in the Antarctic winter mixed layer. *Glob Biogeochem Cyc* **29**: 427–445.
- Smith JM, Casciotti KL, Chavez FP, Francis CA. (2014). Differential contributions of archaeal ammonia oxidizer ecotypes to nitrification in coastal surface waters. *ISME J* **8**: 1704–1714.
- Smith SV, Hollibaugh JT. (1989). Carbon-controlled nitrogen cycling in a marine 'macrocosm': an ecosystem-scale model for managing cultural eutrophication. *Mar Ecol Prog Ser* **52**: 103–109.
- Solórzano L. (1969). Determination of ammonia in natural waters by the phenol hypochlorite method. *Limnol Oceanogr* **14**: 799–801.
- Spang A, Poehlein A, Offre P, Zumbrägel S, Haider S, Rychlik N *et al.* (2012). The genome of the ammonia-oxidizing Candidatus *Nitrososphaera gargensis*: Insights into metabolic versatility and environmental adaptations. *Environ Microbiol* **14**: 3122–3145.
- Strickland JDH, Parsons TR. (1972). *A Practical Handbook of Seawater Analysis*, 2nd edn, vol. 167. Fisheries Research Board of Canada: Ottawa, Canada.
- Tolar BB, King GM, Hollibaugh JT. (2013). An analysis of Thaumarchaeota populations from the Northern Gulf of Mexico. *Front Microbiol* **4**: 72.
- Wada E, Hattori A. (1972). Nitrite distribution and nitrite reduction in deep sea waters. *Deep-Sea Res* **19**: 123–132.
- Ward BB. (2008). Nitrification in marine systems. In: Capone DG, Bronk DA, Mullholland MR, Carpenter E (eds). *Nitrogen in the Marine Environment*, 2 edn. Elsevier: New York, NY, USA, pp 199–261.
- Ward BB. (2011). Nitrification in the ocean. In: Ward B, Arp DJ, Klotz MJ (eds). *Nitrification*. ASM Press: Washington, DC, USA, pp 325–345.
- Williams TJ, Long E, Evans F, DeMaere MZ, Lauro FM, Raftery MJ *et al.* (2012). A metaproteomic assessment of winter and summer bacterioplankton from Antarctic Peninsula coastal surface waters. *ISME J* **6**: 1883–1900.
- Yakimov MM, Cono VL, Denaro R. (2009). A first insight into the occurrence and expression of functional *amoA* and *accA* genes of autotrophic and ammonia-oxidizing bathypelagic Crenarchaeota of Tyrrhenian Sea. *Deep Sea Res II* **56**: 748–754.
- Yakimov MM, Cono VL, Smedile F, DeLuca TH, Juarez S, Giordina S *et al.* (2011). Contribution of crenarchaeal autotrophic ammonia oxidizers to the dark primary production in Tyrrhenian deep waters (Central Mediterranean Sea). *ISME J* **5**: 945–961.
- Yool A, Martin AP, Fernandez C, Clark DR. (2007). The significance of nitrification for oceanic new production. *Nature* **447**: 999–1002.



This work is licensed under a Creative Commons Attribution-NonCommercial-ShareAlike 4.0 International License. The images or other third party material in this article are included in the article's Creative Commons license, unless indicated otherwise in the credit line; if the material is not included under the Creative Commons license, users will need to obtain permission from the license holder to reproduce the material. To view a copy of this license, visit <http://creativecommons.org/licenses/by-nc-sa/4.0/>

Supplementary Information accompanies this paper on The ISME Journal website (<http://www.nature.com/ismej>)